Cation Effects in p-Type Dye Sensitized Solar Cells

Jake M. Evans, Shannon M. McCullough, Taylor M. Moot, Aaron D. Taggart, Ludovic Troian-Gautier, and James F. Cahoon[*]

[*]Corresponding Author

Department of Chemistry, University of North Carolina at Chapel Hill, Chapel Hill, NC 27599-3290, United States

Keywords Cation effects, dye-sensitized solar cell, nickel oxide, p-type metal oxide

ABSTRACT

The performance of dye sensitized solar cells depends on the properties and interactions of three fundamental components: the semiconductor, chromophore, and electrolyte. Performance dependence on electrolyte cation species has not been well studied in p-type systems. The effects of these species in n-type systems are significant, producing large shifts in semiconductor flat band potential, charge transfer kinetics, and open circuit voltage. Modifying the spectator cation has been shown to increase open circuit voltage by over 50% in two common electrolyte systems. A champion open circuit voltage of 351 mV has been achieved, representing a record for the chromophore employed. Our results indicate that applying this knowledge to any p-type dye sensitized solar cell system can yield improvements in important device metrics.

INTRODUCTION

Dye-sensitized solar cells (DSSCs) are a low-cost alternative to traditional solar cells which have received considerable attention since the initial reporting by Grätzel in 1991.[1] The basic components of a DSSC are a semiconductor, a chromophore, and an electrolyte. Upon illumination, the chromophore is excited and is subsequently either reduced (p-type) or oxidized

(n-type) by the semiconductor – typically a metal oxide. NiO and TiO_2 are common choices for p- and n-type devices, respectively.[2-6] Upon relaxation, the chromophore reacts with a redox-active species in the electrolyte which in turn reacts with a counter electrode, completing the circuit. To improve device performance, each of the fundamental components must be optimized. While research in n-type DSSCs has examined all of these components in depth,[5, 7-12] p-type DSSC studies have prioritized the semiconductor and chromophore.[6, 13-16] It is hypothesized that this has contributed to the poor performance of p-DSSCs in relation to their n-type counterparts. This work serves to improve the understanding of the electrolyte in p-DSSCs by examining the impact of spectator metal cations in p-DSSC electrolytes in an effort to increase the performance of such devices.

As spectators to the redox reactions occurring in the electrolyte, cation species are easily overlooked when optimizing electrolyte composition. However, cations in solution are known to have significant impact in TiO_2 n-DSSCs.[7, 8, 17-19] The cations are able to adsorb to electrode surfaces[20], inducing a dipole. This dipole alters the charge equilibrium at the semiconductor-electrolyte interface, causing a shift in the flat band potential (V_{FB}) of that semiconductor[21] as the Fermi level reaches a new equilibrium. In an ideal case, the open circuit voltage (V_{OC}) of a DSSC depends on the potential difference between the Nernstian potential of the redox couple and the Fermi level of the semiconductor.[21] Therefore the V_{OC} can be increased by increasing that difference, either by changing the redox couple or shifting the semiconductor Fermi level (Figure 1). Altering the cation in solution, then, offers a straightforward method for increasing device V_{OC}.

One of the most common electrolyte systems in both p- and n-DSSCs is the Z960 electrolyte utilizing an I^-/I_3^- redox couple.[22] Conveniently, the I^-/I_3^- redox couple's Nernstian

potential is accessible for both n- and p-DSSCs.[22] However, these two systems operate in reverse, with the n-DSSC's Fermi level lying above the I^-/I_3^- Nernstian potential and the p-DSSC's below.[22] One of the most prominent alternatives to I^-/I_3^- is the $Co^{II/III}$ couple. Previous studies have demonstrated the promise of this system[23, 24] and its simplicity minimizes the variables in the experiments. The electrolyte is composed of a perchlorate salt and tris(4,4'-di-tert-butyl-2,2'-dipyridyl) cobalt (II/III) perchlorate – abbreviated as $Co(dtb)^{II/III}$ – dissolved in propylene carbonate. Li^+, Mg^{2+}, and Al^{3+} were selected to test cation effects in the I^-/I_3^- system as their iodide salts were readily available. In the $Co(dtb)^{II/III}$ system, in addition to the previously mentioned cations Na^+, Sr^{2+}, and Ca^{2+} were used, as this would allow for an examination of ionic radius effects and the perchlorate salts were more versatile in electrochemical measurements. A positive charge near the surface will induce a dipole which stabilizes electronic energies, lowering the Fermi level. Therefore, a p-DSSC favors an increase in V_{FB} and an n-DSSC favors a decrease in V_{FB}. A device with higher charged cations in solution would then be expected to have a larger V_{OC}. Nickel oxide will be used as the p-type semiconductor in this study as it is a ubiquitous material for p-DSSCs. The chromophore selected is Dyenamo FP01 (P1), a common organic chromophore used in NiO DSSCs.[15]

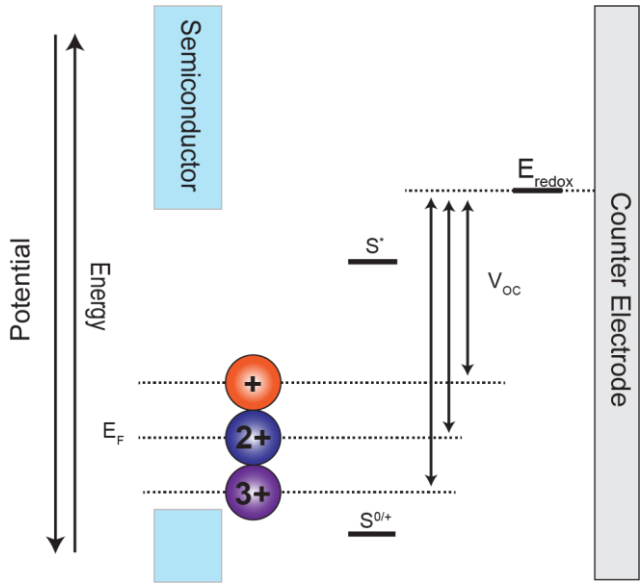

Figure 1. Depiction of Fermi energy shifts as cations of increasing charge are adsorbed to the surface.

RESULTS AND DISCUSSION

To confirm the stated effects of ions on the semiconductor's energetics, Mott-Schottky analysis was performed. Mott-Schottky analysis is an AC impedance technique which measures the capacitance of the working electrode as a function of applied bias at a fixed AC frequency. Capacitance of a film is linked to the V_{FB} through the Mott-Schottky equation (Eq. 1).

Equation 1. $$C^{-2} = \frac{2}{\varepsilon\varepsilon_0 A^2 e N_A}\left(V - V_{FB} - \frac{k_B T}{e}\right)$$

Where C is capacitance, V is potential, k_B is Boltzmann's constant, A is the area of the electrode, e is the fundamental charge of an electron, T is temperature in Kelvin, ε is the dielectric constant of the solution, and ε_0 is the dielectric constant of free space. The inverse square of the capacitance can be plotted against the applied potential to extract V_{FB}. When $C^{-2} = 0$, $V = V_{FB} + kT/e$. Mott-Schottky analysis is most accurate for planar films and thus the trend extracted for the mesoporous films used in this work is more important to consider than the values of V_{FB}.[25] Mott-

Schottky analysis was performed in solutions with different dissolved perchlorate salts using a three-electrode cell using a Ag/AgCl reference electrode, NiO working electrode and Pt mesh counter. The linear region was fit to Eq. 1. V_{FB} is observed to increase with increasing ionic charge (Figure 2A), consistent with reports on TiO_2 cation effects[8,7,18]. Li^+ is observed to have a V_{FB} of -0.25 V vs Ag/AgCl and Na^+ has a more negative V_{FB} of -0.30 V vs Ag/AgCl while alkali earth ions (Sr^{2+}, Ca^{2+}, Mg^{2+}) have much more positive V_{FB}s ranging from -0.16 V to 0.21 V vs Ag/AgCl. The most highly charged ion studied, Al^{3+}, has the most positive V_{FB} at 0.72 V vs Ag/AgCl. As predicted, V_{FB} increases with the increasing charge density of the cation in solution.

This observation has useful implications for the composition of p-DSSC electrolytes. It is common for p-DSSCs to adopt the same electrolyte as n-DSSCs which typically have Li^+ in solution as Li^+ has favorable energetics for an n-DSSC. However, Figure 1 indicates Li^+ is a poor option for p-type systems due to its low flat band potential. Ignoring this effect limits the potential of p-DSSCs. In fact, Li^+ has the lowest observed V_{FB} of any ion besides Na^+. A p-DSSC favors a very positive shift in V_{FB}, which Figure 1 suggests Mg^{2+} and Al^{3+} provide. However, ion charge alone is not the only variable to consider. The size of the ion is also observed to affect the V_{FB}. As ion size increases, charge density decreases. A lower electric field would then be experienced at the surface, resulting in a smaller induced dipole and reduced band bending, observed in Figure 1 as a decrease in V_{FB}. An estimate of the strength of the electric field experienced by the semiconductor can be calculated by treating the ion as a point charge and assuming the ionic radius is the distance between the charge and the surface. Ionic radii are sourced from literature.[26] Comparing the calculated field strength to the V_{FB} (Figure 2) a similar trend is observed, implying electric field strength is an important factor in predicting V_{FB}.

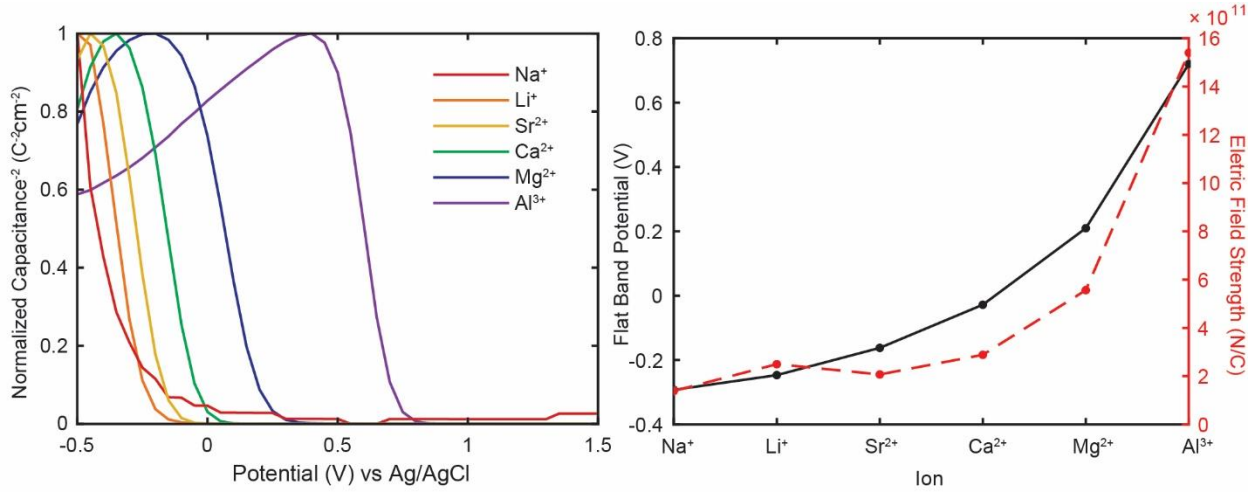

Figure 2. (A) Mott-Schottky curves of mesoporous NiO films in 0.1 M $X(ClO_4)_n$ in acetonitrile where X is the cation of interest and n varies as appropriate to balance charge. Capacitance values are normalized for ease of viewing. From this, (B) flat band potential values are extracted and compared to electric field strength of cations.

Electrochemical impedance spectroscopy (EIS) was used to determine the impact of different cations on interfacial charge transfer. EIS has become an increasingly powerful technique for characterizing DSSCs, and several significant parameters have been quantified using this technique including charge transfer resistances and recombination resistances.[27,28] An equivalent circuit representing a modified double Randles cell (Figure S1) was used to model each device. Nyquist plots are useful for identifying the charge transfer processes present in a system. Nyquist plots were constructed for each device and a representative plot is displayed in Figure 3A. There are two distinct semicircles, indicating there are two charge transfer regimes of significance. The size of these semicircles varies with applied bias. The large dependence of the larger semicircle on applied bias indicates it is linked to the semiconductor interface as the behavior of the Pt counter is unlikely to be significantly altered by a change in potential. Charge

transfer resistance (R_{CT}) and hole lifetime (τ) at the NiO interface were extracted and plotted as a function of applied bias (Figure 3B). These parameters decrease in all systems as bias is increased due to the increase in hole concentration. The values of R_{CT} and τ vary significantly as the cation is changed (Table 1), more so even than applied bias.

Bode plots were constructed for each device at V_{OC} (Figure 3C). The first set of devices analyzed used a Z960-like electrolyte previously reported[6,29] utilizing the I^-/I_3^- couple. Electrolytes had the same composition with the exception of cation identity. The Bode plots for the I^-/I_3^- couple ions have peaks in two distinct frequency ranges. The dependence of these peaks on light intensity was examined to assist in assigning them to processes in the device (Figure S2). The peak at lower frequencies is attributed to charge transfer at the NiO-chromophore-electrolyte interface while the peak at higher frequencies is attributed to the Pt-electrolyte charge transfer. Recombination losses occur at the NiO interface and so the charge transfer resistance is attributed to recombination processes.[27] The MgI_2 electrolyte has a significantly larger peak in the Pt range, indicating more capacitive character. Light intensity testing indicates the NiO charge transfer peak is present in the MgI_2 plot at higher frequency, but is obscured by the Pt peak (Figure S2). This shift to a higher frequency region is indicative of a shorter hole lifetime, but the charge transfer resistance at this interface is 150Ω higher than that of the LiI device, suggesting recombination is a slower process at the NiO interface. The high-frequency peak in the MgI_2 plot is significantly more capacitive than the LiI plot, demonstrating that spectator cations have considerable influence over charge transfer kinetics. The NiO peak in AlI_3 has also shifted to a higher frequency but without a corresponding increase in charge transfer resistance at the NiO interface. In fact, the resistance decreases by 50Ω. Charges are freer to recombine in the AlI_3 electrolyte, contributing to its lower performance.

The $Co(dtb)^{II/III}$ devices were also characterized using EIS. Bode plots at device V_{OC} were again constructed (Figure 3D). Peaks in the Pt region observed in the iodide devices are again much more capacitive, which may be due to the increased charge transfer resistance as discussed previously, but the electrolytes differ to an extent that a direct comparison is difficult. Using the equivalent circuit model charge transfer resistances and hole lifetimes can again be extracted for analysis. Hole lifetimes are observed to increase with increasing ion charge in the $Co(dtb)^{II/III}$ devices but does not appear to appreciably trend with charge density. Calculated hole lifetimes in the iodide devices were on the order of milliseconds but the $Co(dtb)^{II/III}$ devices had values on the order of seconds. The mesoporous nature is most likely hindering the accuracy of these values, but as previously stated, the trend is of greater importance. Charge transfer resistances are considerably higher in the $Co(dtb)^{II/III}$ devices and have much more variation than what was observed in the iodide devices, ranging from a few hundred ohms in NaCo to a few thousand ohms in MgCo. These two observations indicate a much lower rate of recombination at the NiO interface. Charge separation is then more effective and charges can more efficiently move through the cell. The increased charge transfer resistance may also indicate increased difficulty in charge injection by the chromophore which is observed in the *JV* curves as a lower current density. Al^{3+} has a very large feature at low frequency, indicating a drastic change in the capacitance of the device due to a spectator cation. EIS analysis has revealed that ions present in solution have considerable effects on charge transfer kinetics in addition to altering the band bending of the semiconductor.

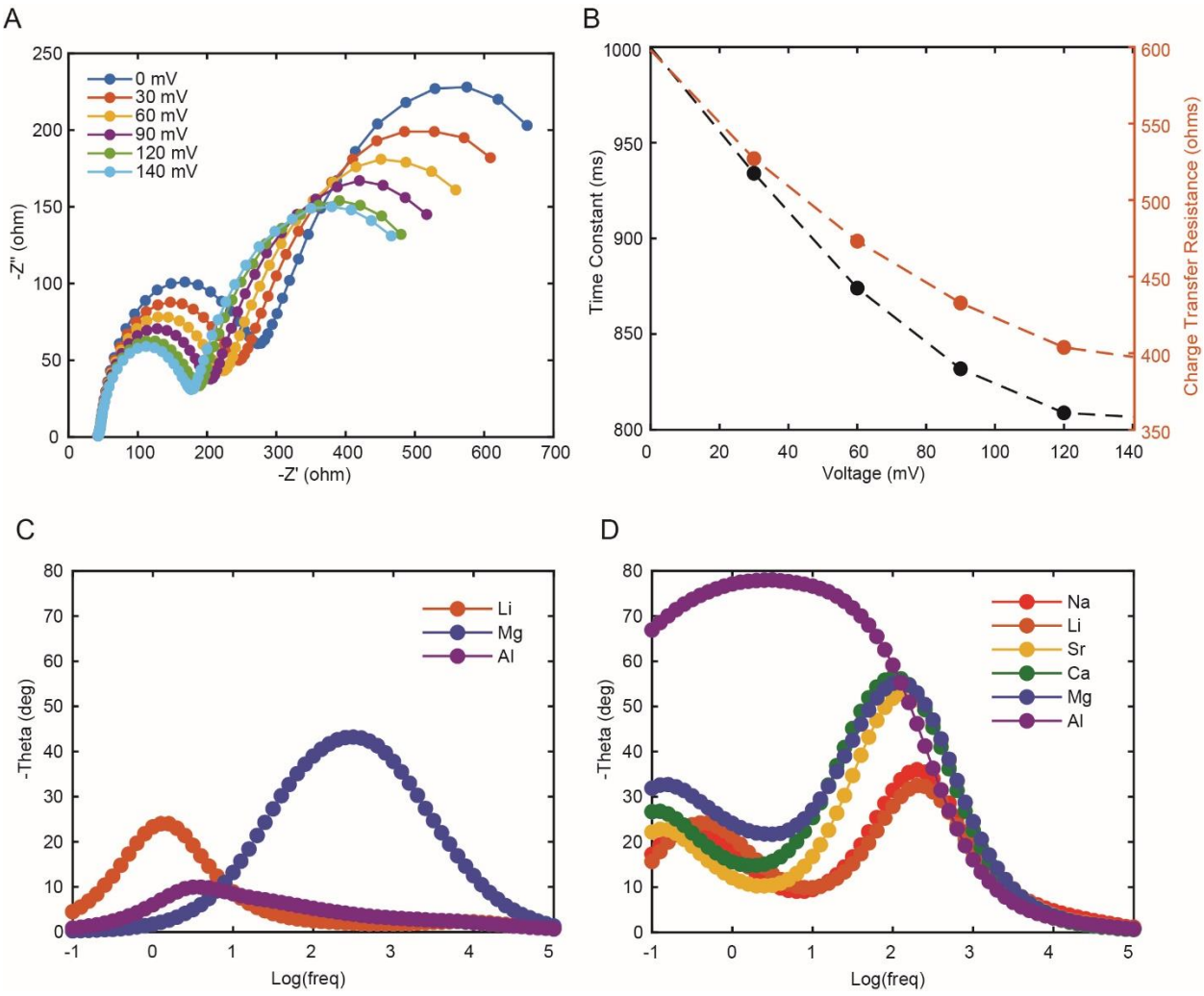

Figure 3. (A) Nyquist plots for DSSC at various applied biases with the 0.1 M Li^+ in $Co(dtb)^{II/III}$ electrolyte. Bias was increased from 0 mV to device V_{OC} (140 mV). (B) The time constant for recombination and charge transfer resistance in (A) were extracted at each potential and plotted. Bode plots for DSSCs using the (C) I^-/I_3^- and (D) $Co(dtb)^{II/III}$ electrolytes.

Table 1. Charge Transfer Parameters at the NiO Interface Extracted from EIS Measurements

Ion/Electrolyte	R_{CT} (ohms)	Time constant (ms)
Li/I	82.82	191.5
Mg/I	233.6	4.800
Al/I	32.31	3.215
Na/Co	450.8	952.9
Li/Co	402.8	809.3
Sr/Co	1384	2999
Ca/Co	3279	4612
Mg/Co	5088	3396
Al/Co	62.32	8.712

Based on electrochemical measurements, devices were fabricated to test whether the predicted V_{OC} increases are observed in solar cells. Current density-voltage (*JV*) characterization was carried out for all devices under one-sun illumination. *JV* characterization is a fundamental technique for measuring the performance of a solar cell. The current of the cell is plotted as a function of applied bias and important device metrics can be extracted from this data with the non-ideal diode equation. The first set of devices tested contained the I^-/I_3^- electrolyte. As the standard Li^+ ion is exchanged for Mg^{2+} the V_{OC} increases substantially, evident in Figure 4 as a 66 mV increase in V_{OC}, a 62% improvement. Short-circuit current density (J_{SC}) does decrease somewhat in the Mg^{2+} electrolyte, and the power conversion efficiency (PCE), a measure of the overall efficiency of the cell, increases by 58%. These improvements confirm the predictions from Figure 1 that Mg^{2+} is a more energetically favorable cation for p-DSSC electrolytes. Figure 1 would then imply that Al^{3+} should produce an even greater Voc and perhaps increase PCE as well. Experiments, though, indicate that devices were negatively affected by the introduction of Al^{3+}. Devices with Al^{3+} substituted for Li^+ had negligible performance (Figure S3). Subsequent experiments determined Al^{3+} caused the chromophore to desorb from the surface (Figure S4), causing the device to fail. The desorption of the dye is thought to be due to the more electrophilic

Al^{3+} out-competing the NiO surface for the carboxylic acid linkers of the chromophore. A bleaching effect was also observed as the NiO film was exposed to the Al solution, similar to previous reports on targeted atomic deposition.[29] These reports note that too much Al on a NiO surface can block charge injection which is also likely affecting the performance of this device. While Al^{3+} proved problematic, Mg^{2+} has been shown to have significant advantages over Li^+ in the traditional Z960-like electrolyte.

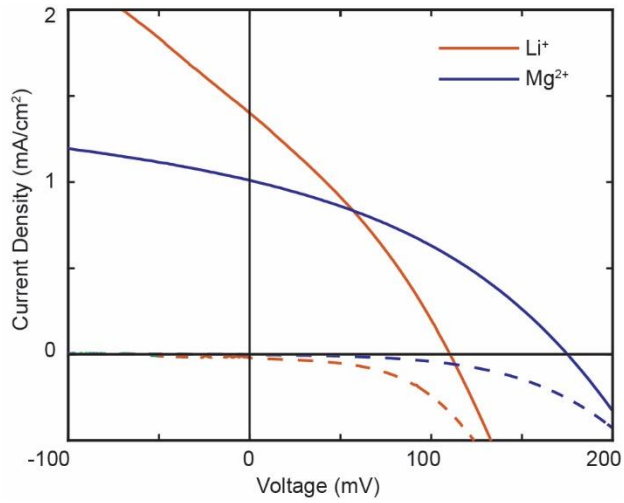

Figure 4. *JV* curves for DSSCs under 1 sun illumination containing Li^+ (orange) and Mg^{2+} (blue) in I^-/I_3^- electrolyte.

With the effect of cations demonstrated using the I^-/I_3^- couple, $Co(dtb)^{II/III}$ based solar cells were characterized next. Figure 5 compares the device performance for p-DSSCs using this system with the same ions as in Figure 4. Average V_{OC} in the $Co(dtb)^{II/III}$ Li^+ devices is 97 mV higher than the I^-/I_3^- Li^+ system. This increase is thought to be primarily due to the change in the Nernstian potential of the redox couple in solution[23]. While this increase is substantial, electrolytes containing Mg^{2+} and Al^{3+} produce devices with even higher V_{OC}s. Mg^{2+} again improved over Li^+ significantly, boosting the average V_{OC} by 106 mV and PCE by 109% when

comparing in the $Co(dtb)^{II/III}$ electrolyte. Compared to the standard Li^+ Z960 system, the Mg^{2+} with the $Co(dtb)^{II/III}$ couple almost triples the average V_{OC} and improves PCE by 250%. While the Al^{3+} devices still have poor J_{SC} and PCE due to dye desorption, a champion V_{OC} of 351 mV is observed and exceeds the largest V_{OC} previously reported using this chromophore[29]. This was the highest V_{OC} produced by any device, consistent with predictions from Figure 1. Tuning of the electrolyte's energetics can thus produce dramatic improvements in device performance. The J_{SC} for Mg^{2+} is higher than Li^+ in this system, though both are lower than the Z960 system. Changing cation species in the electrolyte to favor p-DSSC energetics improved V_{OC} by over 50% in two entirely different electrolytes.

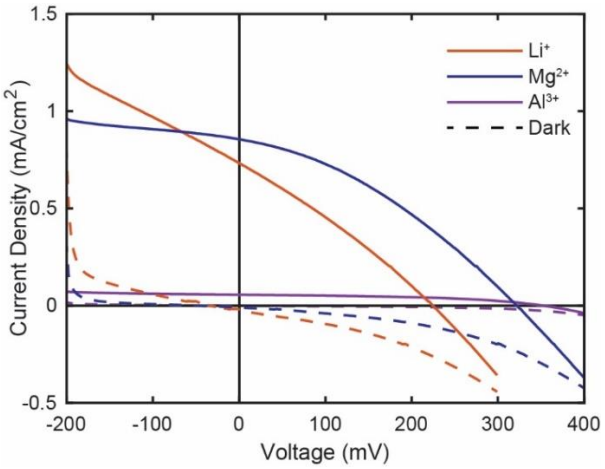

Figure 5. *JV* curves for DSSCs under 1 sun illumination containing Li^+ (orange), Mg^{2+} (blue), and Al^{3+} (violet) in $Co(dtb)^{II/III}$ electrolyte.

Using the information from the previous experiments, the relevance of ionic radius was also examined. Ionic radius has been shown to affect the V_{FB} (Figure 2) so a similar trend was expected in the V_{OC}. *JV* curves were collected for these devices. As predicted, V_{OC} is observed to increase with decreasing atomic radius (Figure 6A and B). However, the effect is small relative to the difference between ions of dissimilar charge. Li^+ has an average V_{OC} of 203±16 mV and Na^+ has an average V_{OC} of 192±10 mV for an average difference of 9 mV. The +2 ions behave

similarly with Sr^{2+}'s average V_{OC} of 286±7 mV, Ca^{2+}'s 298±11, and Mg^{2+}'s 315±21. The difference between the averages is within the error, though champion devices show a clearer trend. Na^{+} and Ca^{2+} have similar ionic radii[26] but Ca^{2+} has an average V_{OC} 106 mV higher. The evidence suggests ionic charge is a much more significant factor than ionic radius for metal cations. However, knowing ion radius affects the potential opens the door to a degree of tuning in the V_{OC} of a DSSC through the electrolyte.

Device performance metrics were summarized for comparison. Ions were arranged from largest and least charged to smallest and most charged in their respective electrolytes. While no clear trend is evident for PCE, J_{SC}, or fill factor, a trend is visible in Voc. As cations become smaller and more positively charged, the V_{OC} increases, consistent with predictions (Figure 6C).

Table 2. Summary of Solar Cell Performance for All Devices

Device (cation/electrolyte)	**J_{SC} (mA/cm2)**	**V_{OC} (mV)**	**Fill Factor (%)**	**Power Conversion Efficiency (%)**
Li/I	1.07 ± 0.26	106 ± 9	31.4 ± 0.8	0.036 ± 0.010
Mg/I	0.92 ± 0.15	172 ± 3	36.0 ± 0.8	0.057 ± 0.008
Na/Co	0.77 ± 0.04	192 ± 10	28.0 ± 0.3	0.042 ± 0.004
Li/Co	0.76 ± 0.02	203 ± 16	28.1 ± 0.3	0.043 ± 0.002
Sr/Co	0.84 ± 0.07	286 ± 7	27.6 ± 2.3	0.066 ± 0.006
Ca/Co	0.64 ± 0.07	298± 11	26.6 ± 4.21	0.052 ± 0.017
Mg/Co	0.85 ± 0.14	315 ± 21	33.8 ± 2.4	0.091 ± 0.016
Al/Co	0.04 ± 0.01	314± 26	44.8 ± 2.8	0.005 ± 0.003

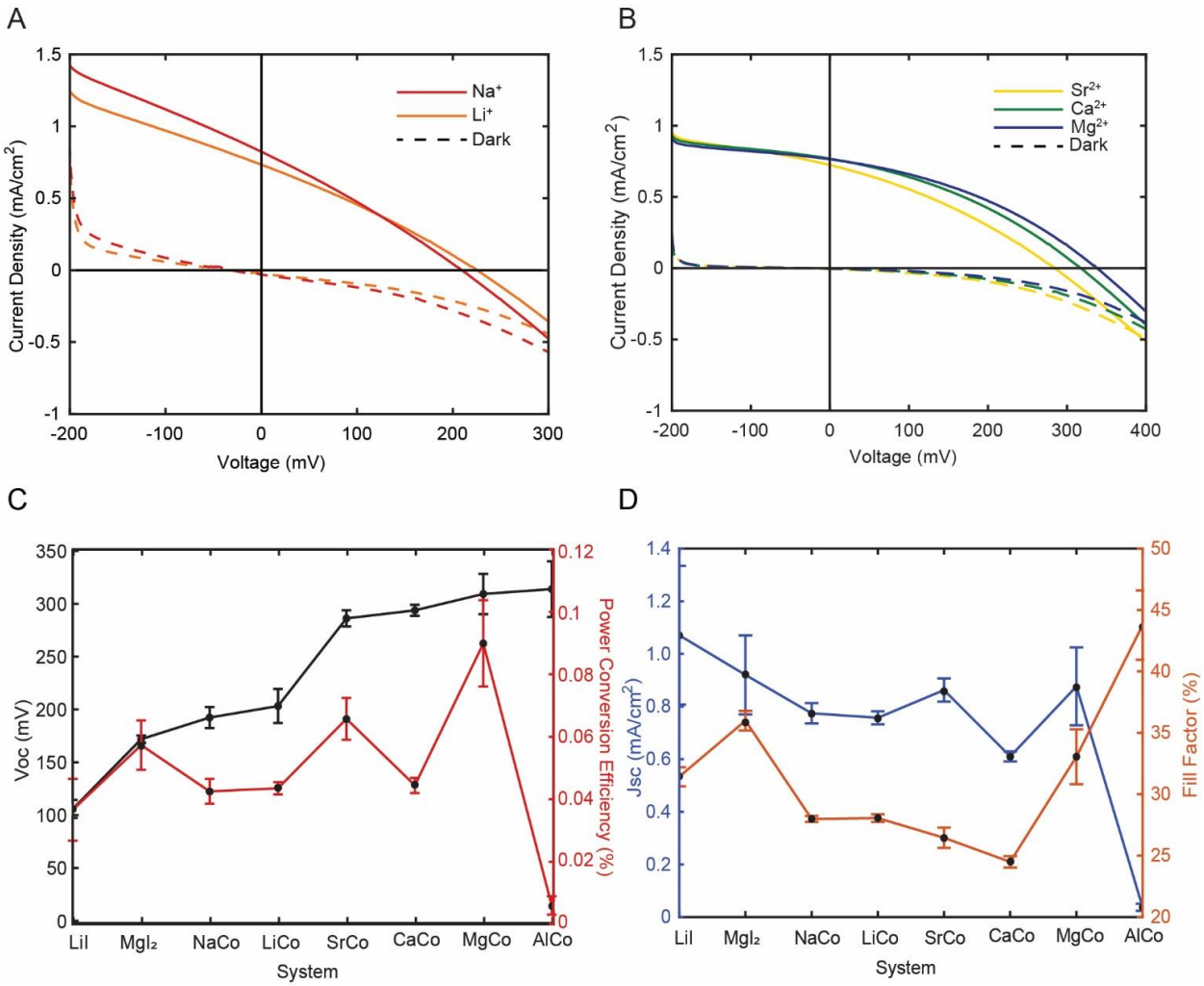

Figure 6. *JV* curves for Co(dtb)$^{II/III}$ DSSCs. Effect of ionic radius on (A) singly and (B) doubly charged ions is examined. Graphical depiction of the effect of cations and redox couple on (C) V_{OC}, PCE, (D) J_{SC}, and fill factor.

CONCLUSIONS AND SUMMARY

Cations in electrolyte solutions have been demonstrated to have significant effects on device energetics. Spectator cations induce a dipole on the semiconductor surface, alter charge transfer kinetics, and change the performance metrics of solar cells. This analysis has revealed the standard Li^+ ion used in the field to be inferior to other choices, most notably Mg^{2+}. Selecting the most favorable option has been demonstrated to yield great improvements in performance.

The effects were consistent between two entirely different electrolytes. Additionally, considering the energetics of both the redox couple and the cations produced devices which had almost three-fold increases in V_{OC} and PCE. Impedance measurements also show the cations can radically alter the lifetime of charges and the resistance of charge transfer between interfaces. It is then essential for spectator cations to be considered when designing p-type DSSC electrolytes.

EXPERIMENTAL

Materials and Reagents

Acetonitrile (99.6%), iodine (>99.99%), lithium iodide (99.9%), lithium perchlorate (>95.0%), calcium perchlorate tetrahydrate (99%), magnesium iodide (98%), magnesium perchlorate (ACS reagent grade), aluminum iodide (>95%), aluminum perchlorate nonahydrate (98%), α-terpineol (anhydrous), and ethyl cellulose (300 cP viscosity) were all purchased from Sigma-Aldrich. Strontium perchlorate trihydrate (98%) and anhydrous sodium perchlorate (>98%) were purchased from Alfa Aesar. Absolute ethanol was purchased from Fisher Scientific. NiO nanoparticles (product #28N-0801) were purchased from Inframat Advanced Materials. 1,3-dimethylimidazolium iodide and 25 μm thick Surlyn polymer was purchased from Solaronix. P1 chromophore was purchased from Dynamo. All chemicals were used as received. Fluorine-doped tin oxide (FTO) glass (TEC 15 Ω·cm2) was purchased from Hartford glass and cleaned with typical organic solvents and sonication.

Tris(4,4’-di-tert-butyl-2,2’-dipyridyl) cobalt (II/III) perchlorate was synthesized according to previously published methods.[30]

NiO Paste Preparation

NiO spin coating paste was prepared using a literature method with Inframat NiO nanoparticles and standard homogenization techniques.[31]

Electrolyte Preparation

Iodide electrolytes were prepared by dissolving solid I_2 in acetonitrile to produce a 5 mM solution. A tenfold excess of an iodide salt (LiI, MgI_2, or AlI_3) was then added to yield a solution that is 5 mM in iodine and 50 mM in the salt. The dissolution of AlI_3 in acetonitrile is very exothermic so it must be added slowly and the glassware was placed in an ice bath. It also reacts vigorously with water so great care must be taken to avoid contact with water.

$Co(dtb)^{II/III}$ solutions were prepared by dissolving 0.1 mmol $Co(dtb)^{II}$ and 0.1 mmol $Co(dtb)^{III}$ in 1 mL propylene carbonate to produce a solution 0.1 M in both $Co(dtb)^{II}$ and $Co(dtb)^{III}$. The perchlorate salt of interest was then added to produce a 0.1 M solution. Note that the perchlorate salts would degrade the electrolyte over time so they must be prepared on the same day as testing. Perchlorate salts are powerful oxidizers and have been known to be explosive so they should be handled with care.

Solar Cell Fabrication

NiO paste was applied to FTO glass via spin-coating. Films were then annealed in a humidity-controlled furnace at 450 °C for 40 minutes. Annealed films were submerged in a 0.3 mM solution of P1 dye for 1 hour. Platinum counter electrodes were fabricated by drop-casting 5 mM chloroplatinic acid solution in isopropanol on FTO glass with a sandblasted hole. The alcohol was allowed to evaporate and then films were annealed at 380 °C for 30 minutes. DSSCs were sandwiched with 25 μm thick Surlyn polymer gasket using a heating apparatus. Sandwiched devices were vacuum-backfilled with electrolyte and then sealed with Surlyn and microscope coverslip.

Solar Cell Characterization

Devices were illuminated using a Newport Oriel 94021A solar simulator calibrated to AM 1.5 with a certified reference Newport 91150 V solar cell before each use. Electrochemical measurement was performed with a Keithley 2636A SourceMeter.

Electrochemical Analysis

NiO electrodes were prepared as previously stated. Exposed FTO was masked with Kapton tape. Mott-Schottky tests were performed using a CH Instruments 604 E potentiostat at 100 Hz utilizing a Ag/AgCl reference electrode, NiO working electrode, and Pt mesh counter.

Electrochemical impedance spectroscopy was performed using a Gamry PCI4-G750-51087 potentiostat. Devices were illuminated using a Newport Oriel 91191-1000 solar simulator calibrated to AM 1.5.

References

1. O'Regan, B.; Grätzel, M., A low-cost, high-efficiency solar cell based on dye-sensitized colloidal TiO2 films. *Nature* **1991,** *353*, 737.
2. Grätzel, M., Dye-sensitized solar cells. *Journal of Photochemistry and Photobiology C: Photochemistry Reviews* **2003,** *4* (2), 145-153.
3. He, J.; Lindström, H.; Hagfeldt, A.; Lindquist, S.-E., Dye-Sensitized Nanostructured p-Type Nickel Oxide Film as a Photocathode for a Solar Cell. *The Journal of Physical Chemistry B* **1999,** *103* (42), 8940-8943.
4. Bandara, J.; Weerasinghe, H., Solid-state dye-sensitized solar cell with p-type NiO as a hole collector. *Solar Energy Materials and Solar Cells* **2005,** *85* (3), 385-390.
5. Crossland, E. J. W.; Noel, N.; Sivaram, V.; Leijtens, T.; Alexander-Webber, J. A.; Snaith, H. J., Mesoporous TiO2 single crystals delivering enhanced mobility and optoelectronic device performance. *Nature* **2013,** *495*, 215.
6. Flynn, C. J.; Oh, E. E.; McCullough, S. M.; Call, R. W.; Donley, C. L.; Lopez, R.; Cahoon, J. F., Hierarchically-Structured NiO Nanoplatelets as Mesoscale p-Type Photocathodes for Dye-Sensitized Solar Cells. *The Journal of Physical Chemistry C* **2014,** *118* (26), 14177-14184.
7. O'Donnell, R. M.; Sampaio, R. N.; Barr, T. J.; Meyer, G. J., Electric Fields and Charge Screening in Dye Sensitized Mesoporous Nanocrystalline TiO2 Thin Films. *The Journal of Physical Chemistry C* **2014,** *118* (30), 16976-16986.
8. Kelly, C. A.; Farzad, F.; Thompson, D. W.; Stipkala, J. M.; Meyer, G. J., Cation-Controlled Interfacial Charge Injection in Sensitized Nanocrystalline TiO2. *Langmuir* **1999,** *15* (20), 7047-7054.
9. Maitani, M. M.; Tsukushi, Y.; Hansen, N. D. J.; Sato, Y.; Mochizuki, D.; Suzuki, E.; Wada, Y., Low-temperature annealing of mesoscopic TiO2 films by interfacial microwave heating applied to efficiency improvement of dye-sensitized solar cells. *Solar Energy Materials and Solar Cells* **2016,** *147*, 198-202.
10. Sigdel, S.; Dubey, A.; Elbohy, H.; Aboagye, A.; Galipeau, D.; Zhang, L.; Fong, H.; Qiao, Q., Dye-sensitized solar cells based on spray-coated carbon nanofiber/TiO2 nanoparticle composite counter electrodes. *Journal of Materials Chemistry A* **2014,** *2* (29), 11448-11453.
11. Wang, H.; Liu, Y.; Li, M.; Huang, H.; Xu, H. M.; Hong, R. J.; Shen, H., *Multifunctional TiO2 nanowires-modified nanoparticles bilayer film for 3D dye-sensitized solar cells*. 2010; Vol. 4, p 1166-1169.
12. Dell'Orto, E.; Raimondo, L.; Sassella, A.; Abbotto, A., Dye-sensitized solar cells: spectroscopic evaluation of dye loading on TiO2. *Journal of Materials Chemistry* **2012,** *22* (22), 11364-11369.
13. Wei, L.; Jiang, L.; Yuan, S.; Ren, X.; Zhao, Y.; Wang, Z.; Zhang, M.; Shi, L.; Li, D., Valence Band Edge Shifts and Charge-transfer Dynamics in Li-Doped NiO Based p-type DSSCs. *Electrochimica Acta* **2016,** *188*, 309-316.
14. Dini, D.; Halpin, Y.; Vos, J. G.; Gibson, E. A., The influence of the preparation method of NiOx photocathodes on the efficiency of p-type dye-sensitized solar cells. *Coordination Chemistry Reviews* **2015,** *304-305*, 179-201.
15. Wood, C. J.; Summers, G. H.; Clark, C. A.; Kaeffer, N.; Braeutigam, M.; Carbone, L. R.; D'Amario, L.; Fan, K.; Farré, Y.; Narbey, S.; Oswald, F.; Stevens, L. A.; Parmenter, C.

D. J.; Fay, M. W.; La Torre, A.; Snape, C. E.; Dietzek, B.; Dini, D.; Hammarström, L.; Pellegrin, Y.; Odobel, F.; Sun, L.; Artero, V.; Gibson, E. A., A comprehensive comparison of dye-sensitized NiO photocathodes for solar energy conversion. *Physical Chemistry Chemical Physics* **2016,** *18* (16), 10727-10738.
16. Click, K. A.; Beauchamp, D. R.; Garrett, B. R.; Huang, Z.; Hadad, C. M.; Wu, Y., A double-acceptor as a superior organic dye design for p-type DSSCs: high photocurrents and the observed light soaking effect. *Physical Chemistry Chemical Physics* **2014,** *16* (47), 26103-26111.
17. Redmond, G.; Fitzmaurice, D., Spectroscopic determination of flatband potentials for polycrystalline titania electrodes in nonaqueous solvents. *The Journal of Physical Chemistry* **1993,** *97* (7), 1426-1430.
18. Wang, H.; Peter, L. M., Influence of Electrolyte Cations on Electron Transport and Electron Transfer in Dye-Sensitized Solar Cells. *The Journal of Physical Chemistry C* **2012,** *116* (19), 10468-10475.
19. Jeanbourquin, X. A.; Li, X.; Law, C.; Barnes, P. R. F.; Humphry-Baker, R.; Lund, P.; Asghar, M. I.; O'Regan, B. C., Rediscovering a Key Interface in Dye-Sensitized Solar Cells: Guanidinium and Iodine Competition for Binding Sites at the Dye/Electrolyte Surface. *Journal of the American Chemical Society* **2014,** *136* (20), 7286-7294.
20. Liu, Y.; Hagfeldt, A.; Xiao, X.-R.; Lindquist, S.-E., Investigation of influence of redox species on the interfacial energetics of a dye-sensitized nanoporous TiO2 solar cell. *Solar Energy Materials and Solar Cells* **1998,** *55* (3), 267-281.
21. Walter, M. G.; Warren, E. L.; McKone, J. R.; Boettcher, S. W.; Mi, Q.; Santori, E. A.; Lewis, N. S., Solar Water Splitting Cells. *Chemical Reviews* **2010,** *110* (11), 6446-6473.
22. Boschloo, G.; Hagfeldt, A., Characteristics of the Iodide/Triiodide Redox Mediator in Dye-Sensitized Solar Cells. *Accounts of Chemical Research* **2009,** *42* (11), 1819-1826.
23. Gibson, E. A.; Smeigh, A. L.; Le Pleux, L.; Fortage, J.; Boschloo, G.; Blart, E.; Pellegrin, Y.; Odobel, F.; Hagfeldt, A.; Hammarström, L., A p-Type NiO-Based Dye-Sensitized Solar Cell with an Open-Circuit Voltage of 0.35 V. *Angewandte Chemie International Edition* **2009,** *48* (24), 4402-4405.
24. Giribabu, L.; Bolligarla, R.; Panigrahi, M., Recent Advances of Cobalt(II/III) Redox Couples for Dye-Sensitized Solar Cell Applications. *The Chemical Record* **2015,** *15* (4), 760-788.
25. Gelderman, K.; Lee, L.; Donne, S. W., Flat-Band Potential of a Semiconductor: Using the Mott–Schottky Equation. *Journal of Chemical Education* **2007,** *84* (4), 685.
26. Shannon, R., Revised effective ionic radii and systematic studies of interatomic distances in halides and chalcogenides. *Acta Crystallographica Section A* **1976,** *32* (5), 751-767.
27. Huang, Z.; Natu, G.; Ji, Z.; Hasin, P.; Wu, Y., p-Type Dye-Sensitized NiO Solar Cells: A Study by Electrochemical Impedance Spectroscopy. *The Journal of Physical Chemistry C* **2011,** *115* (50), 25109-25114.
28. Wang, Q.; Moser, J.-E.; Grätzel, M., Electrochemical Impedance Spectroscopic Analysis of Dye-Sensitized Solar Cells. *The Journal of Physical Chemistry B* **2005,** *109* (31), 14945-14953.
29. Flynn, C. J.; McCullough, S. M.; Oh, E.; Li, L.; Mercado, C. C.; Farnum, B. H.; Li, W.; Donley, C. L.; You, W.; Nozik, A. J.; McBride, J. R.; Meyer, T. J.; Kanai, Y.; Cahoon, J. F., Site-Selective Passivation of Defects in NiO Solar Photocathodes by Targeted Atomic Deposition. *ACS Applied Materials & Interfaces* **2016,** *8* (7), 4754-4761.

30. Nelson, J. J.; Amick, T. J.; Elliott, C. M., Mass Transport of Polypyridyl Cobalt Complexes in Dye-Sensitized Solar Cells with Mesoporous TiO2 Photoanodes. *The Journal of Physical Chemistry C* **2008,** *112* (46), 18255-18263.
31. Ito, S.; Murakami, T. N.; Comte, P.; Liska, P.; Grätzel, C.; Nazeeruddin, M. K.; Grätzel, M., Fabrication of thin film dye sensitized solar cells with solar to electric power conversion efficiency over 10%. *Thin Solid Films* **2008,** *516* (14), 4613-4619.